Hydro-magnetic double-diffusive natural convection in a rectangular enclosure with imposing an inner heat source or sink

Mohamed A. Teamah
Mechanical Eng. Dept., Faculty of Eng., Alexandria University, Alexandria, Egypt
E-mail: mteamah@yahoo.com

Finite-volume is used to predict numerically the characteristics of hydromagnetic double-diffusive convective flow of air in a rectangular enclosure with the upper and lower surfaces being insulated and impermeable. Constant temperatures and concentration are imposed along the left and right walls of the enclosure. In addition, a uniform magnetic field is applied in a horizontal direction. Laminar regime is considered under steady state condition. The transport equations for continuity, momentum, energy and spices transfer are solved. The numerical results are reported for the effect of thermal Rayleigh number, heat generation or absorption coefficient and the Hartmann number on the contours of streamline, temperature, and concentration as well as the dimensionless density. In addition, the predicted results for the average Nusselt and Sherwood numbers are presented and discussed for various parametric conditions. This study was done for constant aspect ratio A=2, Lewis number Le=1 and Prandtl number Pr=0.7. The study covers ranges for $10^3 \leq Ra_T \leq 10^6$, $0 \leq Ha \leq 200$, $-50 \leq \varphi \leq 25$ and $-10 \leq N \leq 10$.

البحث يحتوى على دراسه عددية للحمل الرقائقى الحر ثنائى الانتشار (انتقال الحرارة والكتلة) فى حيز على شكل مستطيل . وقد فرض ان الجدران الرأسية ذات درجات حرارة وتركيز ثابت بينما الأسطح الافقية معزوله وغير نافذة. ويتعرض هذا الحيز الى مجال مغناطيسى او كهربى افقى. ويحتوى هذا الحيز على مصدر لتوليد الطاقة الحرارية او امتصاصها حيث يستخدم هذا فى العديد من التطبيقات الهندسية مثل الاسالة والتجميد والكريستال وصناعة السبائك فائقة التوصيل الكهربى التى تمثل اساس الصناعة الالكترونية الحديثة للترانزستور والليزر واجهزة الميكروويف والدوائر المتكاملة وأجهزة الذاكرة فى الحاسبات الالكترونية وغيرها.
وقد تم استنباط نموذج رياضى وتم حلة عدديا، وقد غطى هذا البحث مدى واسعا لرقم رالى الحرارى من ١٠^٣ الى ١٠^٦ ورقم هارتمان من صفر الى ٢٠٠ وقد شملت الدراسة حالتى التوليد والامتصاص الحرارى وفد تغير هذا المعامل من –٥٠ (امتصاص) الى ٢٥ (توليد) وقد تم ايضا دراسة كل من حالة اتحاد وتضاد اتجاة قوي الطفو وتغيرت النسبة بين قوتى الطفو من -١٠ الى ١٠ .
وقد اجرى البحث عند ثبات كل من رقم لويس عند ١ ورقم براندل عند ٠,٧ وارتفاع المستطيل ضعف طول قاعدتة وقد تم دراسة تأثير العوامل السابقة على كل من خطوط السريان وخطوط ثبات الكثافة ودرجة الحرارة والتركيزداخل الحيز وتأثيرهم ايضا على كل من رقم نوسلت ورقم شيروود الموضعى والمتوسط وقد عقدت مقارنة مع الابحاث السابقة وقد اظهرت المقارنة توافق مقبول مع الابحاث المنشورة.

Keyword: Double-diffusive flow, Heat and mass transfer, Magnetic field, Heat generation, Heat absorption

1. Introduction

Natural convection is of a great importance in many industrial applications. Convection plays a dominant role in crystal growth in which it affects the fluid-phase composition and temperature at the phase interface. It is the foundation in modern electronics industry to produce pure and perfect crystals to make transistors, lasers rods, microwave devices, infrared detectors, memory devices, and integrated circuits. Natural convection adversely affects local growth conditions and enhances the overall transport rate. In addition, the application of a magnetic field in various research areas has significantly increased in recent years. The development of super-conducting magnets has allowed the generation of magnetic fields up to 20 T (or higher with hybrid magnets), as reported by Ujihara et al. [1]

Many investigators studied the simple rectangular and square cavities with temperature gradient experimentally and numerically. A good review was reported by Ostrach [2]. A complicated inclined cavity with inner heat generation was studied numerically by Acharya and Goldstein [3]. They introduced two Rayleigh numbers. The first is internal Rayleigh Ra_i, based on the rate of heat generation and external Rayleigh number Ra_E, based on temperature difference. Their study covered a range for Ra_i from 10^4 to 10^7 and Ra_E from 10^3 to 10^6, and cavity inclination angle from 30^o to 90^o. Also, Rahman and Sharif [4] studied numerically the same geometry with heated bottom and cooled top surfaces and insulated sides. In their study, both Ra_I and Ra_E were 2×10^5 and the aspect ratio ranged from 0.25 to 4. They found that for $Ra_E/Ra_I > 1$, the convective flow and heat transfer were almost the same as that in a cavity without internal heat generating fluid and they observed similar results as in Acharya and Goldstein [3]. Oztop and Bilgen [5] studied numerically the presence of a partial divider in a differentially heated enclosure containing heat generating fluid which adds an additional dynamic effect to overall convection characteristics. Their study covered both Ra_i and Ra_E over a range from 10^3 to 10^6. Also, they studied the various partial divider geometry and position. In their study they used a modified version of the general-purpose SAINTS software (Software for Arbitrary Integration of Navier–Stokes Equation with a Turbulence and Porous Media Simulator). SAINTS makes use of the SIMPLE algorithm explained by Patankar [6].

One of the effective means practiced in industry for thermally induced melt flow control is magnetic damping, which is derived from the interaction between an electrically conducting melt flow and an applied magnetic field to generate an opposing Lorentz force to the convective flows in the melt. The damping effect depends on the strength of the applied magnetic field and its orientation with respect to the convective flow direction. Substantial theoretical and numerical work, thus far, has appeared on magnetic damping for natural convection as reported by Shu et al. [7]. Ozoe and Okada [8] conducted a numerical analysis of the magnetic damping effect in a cubic cavity with two vertical walls at different temperatures. They found that the strongest damping effect is achieved with the magnetic field applied perpendicular to the hot wall. This is consistent with the work of Alboussie`re et al. [9] who used an asymptotic approach, and found that for a rectangular box, the damping effect is the weakest when the applied magnetic field is horizontal and parallel to the hot wall. Wakayama [10] reported a jet flow of nitrogen gas in a decreasing magnetic field as another example of this magnetic force. Bai et al. [11] made a numerical analysis for this study. Tagawa et al. [12] employed a similar way to Boussinesq approximation for this magnetic force and carried out numerical analysis for natural convection of air in a cubic enclosure. Kaneda et al. [13] studied the natural convection in a cube enclosure filled with air. The cube was heated from above and cooled from bottom and the air was driven by a magnetic force. Xu et al. [14] studied experimentally the thermally induced convection of molten gallium in magnetic fields.

During the magnetic liquid encapsulated Czochralski (MLEC) growth of compound semiconductor crystals, a single-crystal seed is lowered through the encapsulate which initiates solidification and crystal growth begins in the presence of an externally applied magnetic field. Morton et al. [15] presented a model of dopant transport during the MLEC process. Previous researchers have investigated the effect of a steady magnetic field on two-dimensional natural convection in rectangular enclosures. Kuniholm and Ma [16] used an asymptotic analysis in order to investigate the interaction between the melt and the encapsulant in a rectangular enclosure with strong magnetic fields. Yang and Ma [17] studied natural convection in a liquid encapsulated molten semiconductor with a horizontal magnetic field numerically. Recently, Wang and co-workers [18-21] conducted very strong series of numerical researches in different methods of crystal growth with electric and magnetic fields in alloys manufacture.

Nishimura et al. [22] studied numerically the oscillatory double-diffusive convection in a rectangular enclosure with combined horizontal temperature and concentration gradients. In their study the following conditions were considered thermal Rayleigh number $=10^5$, Prandtl number = 1, Lewis number= 2, aspect ratio=2 and buoyancy ratio from 0.8 to 2.0. They concluded that the oscillatory double-diffusive convection with the secondary cell flow structure occurs for a certain range of buoyancy ratio from N = 1.044 to 1.122. Chamkha and Al-Naser [23] studied numerically the hydromagnetic double-diffusive convection in a rectangular enclosure with opposing temperature and concentration gradients. Their cavity and conditions were similar to that of Nishimura [22] but they imposed magnetic field and heat generation. They found that the effect of the magnetic field reduced the heat transfer and fluid circulation within the enclosure. Also, they concluded that the average Nusselt number increased owing to the presence of a heat sink while it decreased when a heat source was present. And they reported that the periodic oscillatory behavior in the stream function inherent in the problem was decayed by the presence of the magnetic field. This decay in the transient oscillatory behavior was speeded up by the presence of a heat source. Chamkha and Al-Naser [24] extended their previous work by changing the boundary conditions of vertical walls to be at constant heat and mass fluxes.

Nishimura [22] found an oscillatory flow in double-diffusive convection in a rectangular enclosure. Chamkha and Al-Naser [23] concluded that the magnetic field damped the oscillatory flow for thermal Rayleigh number Ra_T=10^5. The aim of the present study is to explore an existence of oscillatory flow at high thermal Rayleigh number and studying the effect of magnetic field on it. Moreover, study the effect of thermal Rayleigh number, the buoyancy ratio, Hartmann number and the heat generation or absorption coefficient on the heat and mass transfer in the enclosure.

2. Mathematical model

The schematic of the system under consideration is shown in fig. 1. The temperatures T_h and T_c are uniformly imposed along the vertical walls. The top and bottom surfaces are assumed to be adiabatic and impermeable. The left wall is the source for both heat and mass. A magnetic field with uniform strength B_0 is applied in the horizontal direction. Also, the enclosure is filled with a binary mixture of gas. The fluid is assumed to be incompressible, Newtonian, heat generating or absorbing and viscous. Both the viscous dissipation and magnetic dissipation are assumed to be negligible. The Boussinesq approximation eq. (1) with opposite and compositional buoyancy forces is used for the body force terms in the momentum equations.

$$\rho = \rho_o \left[1 - \beta_T (T - T_c) - \beta_S (c - c_l) \right]. \tag{1}$$

The governing equations for the problem under consideration are based on the balance laws of mass, linear momentum, thermal energy and concentration in two dimensions steady state. Following the previous assumptions, these equations can be written in dimensional form as;

$$\frac{\partial u}{\partial x} + \frac{\partial v}{\partial y} = 0 , \tag{2}$$

$$u \frac{\partial u}{\partial x} + v \frac{\partial u}{\partial y} = - \frac{1}{\rho} \frac{\partial p}{\partial x} + \upsilon \left[\frac{\partial^2 u}{\partial x^2} + \frac{\partial^2 u}{\partial y^2} \right], \tag{3}$$

$$u \frac{\partial v}{\partial x} + v \frac{\partial v}{\partial y} = - \frac{1}{\rho} \frac{\partial p}{\partial y} + \upsilon \left[\frac{\partial^2 v}{\partial x^2} + \frac{\partial^2 v}{\partial y^2} \right] + g\beta_T (T - T_c) - g\beta_c (c - c_l) + \frac{\sigma B_o^2}{\rho} v , \tag{4}$$

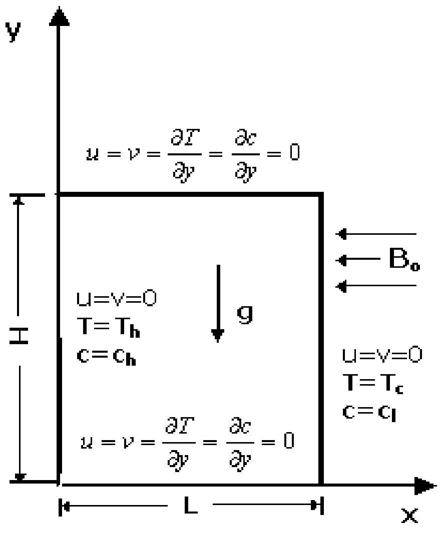

Fig. 1. A schematic diagram for the problem with boundary conditions.

$$u\frac{\partial T}{\partial x}+v\frac{\partial T}{\partial y}=\alpha\left[\frac{\partial^2 T}{\partial x^2}+\frac{\partial^2 T}{\partial y^2}\right]+\frac{Q_o}{\rho C_p}\left(T-T_c\right), \quad (5)$$

$$u\frac{\partial c}{\partial x}+v\frac{\partial c}{\partial y}=D\left[\frac{\partial^2 c}{\partial x^2}+\frac{\partial^2 c}{\partial y^2}\right]. \quad (6)$$

Where B_o is the magnetic induction vector in Tesla, N/(Amp.m^2), σ is the electrical conductivity; Amp.m/Volt, Q_o, heat generation or absorption coefficient, Watt/m^3.°C, and D is the mass diffusivity, m^2/s. The boundary conditions are;

$u=v=0.0$, $T=T_h$ and $c=c_h$., at $x=0$
$u=v=0.0$, $T=T_c$ and $c=c_l$., at $x=L$

and at y=0 and y=H

$$u=v=\frac{\partial T}{\partial y}=\frac{\partial c}{\partial y}=0,$$

and introducing the following dimensionless groups for the governing equations,

$$X=\frac{x}{L},\ Y=\frac{y}{L},\ U=\frac{uL}{\alpha},\ V=\frac{vL}{\alpha},$$

$$P=\frac{pL^2}{\rho_o*\alpha^2},\ \theta=\frac{T-T_c}{T_h-T_c}\ \text{and}\ C=\frac{c-c_l}{c_h-c_l}. \quad (7)$$

A set of governing equations is obtained as:

$$\frac{\partial U}{\partial X}+\frac{\partial V}{\partial Y}=0. \quad (8)$$

$$U\frac{\partial U}{\partial X}+V\frac{\partial U}{\partial Y}=-\frac{\partial P}{\partial X}+\Pr\left[\frac{\partial^2 U}{\partial X^2}+\frac{\partial^2 U}{\partial Y^2}\right]. \quad (9)$$

$$U\frac{\partial V}{\partial X}+V\frac{\partial V}{\partial Y}=-\frac{\partial P}{\partial Y}+\Pr\left[\frac{\partial^2 V}{\partial X^2}+\frac{\partial^2 V}{\partial Y^2}\right]+Ra_T\Pr\left[\theta-NC\right]+Ha^2\Pr\times V. \quad (10)$$

$$U\frac{\partial \theta}{\partial X}+V\frac{\partial \theta}{\partial Y}=\left[\frac{\partial^2 \theta}{\partial X^2}+\frac{\partial^2 \theta}{\partial Y^2}\right]+\varphi\times\theta. \quad (11)$$

$$U\frac{\partial C}{\partial X}+V\frac{\partial C}{\partial Y}=\frac{1}{Le}\left[\frac{\partial^2 C}{\partial X^2}+\frac{\partial^2 C}{\partial Y^2}\right]. \quad (12)$$

Where, Pr is the Prandtl number, Ra_T is the thermal Rayleigh number, N is the ratio between solutal Rayleigh number and thermal Rayleigh number$=[\beta_s(c_h-c_l)]/[\beta_T(T_h-T_c)]$, Ha is the Hartmann number$=B_oL\sqrt{\sigma/\mu}$, Φ is the dimensionless heat generation or absorption coefficient$=\left(Q_oL^2\right)/\left(\rho c_p\alpha\right)$, and Le is the Lewis number.

The dimensionless boundary conditions are

$U=V=0.0$, $\theta=1$ and $C=1$, at $X=0$
$U=V=\theta=C=0.0$, at $X=1$

and at Y=0 and at Y= Aspect ratio

$$U=V=\frac{\partial \theta}{\partial Y}=\frac{\partial C}{\partial Y}=0. \quad (13)$$

2.1. Nusselt number calculation

Equating the heat transfer by convection to the heat transfer by conduction at hot wall;

$$h\ \Delta T=-k\left(\frac{\partial T}{\partial x}\right)_{x=0}. \quad (14)$$

Introducing the dimensionless variables, defined in eq. (7), into eq. (14), gives:

$$Nu_l=-\left(\frac{\partial \theta}{\partial X}\right)_{X=0}. \quad (15)$$

The average Nusselt number is obtained by integrating the above local Nusselt number over the vertical wall;:

$$Nu=-\frac{1}{A}\int_0^A\left(\frac{\partial \theta}{\partial X}\right)_{X=0}dY. \quad (16)$$

2.2. Sherwood number calculation

Equating the extracted mass transfer by convection to the added mass transfer to the cavity gives:

$$h_s\Delta c=-D\left(\frac{\partial c}{\partial x}\right)_{x=0}. \quad (17)$$

Introducing the dimensionless variables, defined in eq. (7), into eq. (14), gives:

$$Sh_l = -\left(\frac{\partial C}{\partial X}\right)_{X=0} \quad . \tag{18}$$

The average Sherwood number is obtained by integrating the above local Sherwood number over the vertical wall:

$$Sh = -\frac{1}{A}\int_0^A \left(\frac{\partial C}{\partial X}\right)_{X=0} dY \quad . \tag{19}$$

3. Solution procedure

The governing equations were solved using the finite volume technique developed by Patankar [6]. This technique was based on the discretization of the governing equations using the central difference in space. The number of nodes used was checked. Through out this study, the number of grids (42×122) was used. The 42 grid points in X-direction were enough to resolve the thin boundary layer near the vertical walls. A uniform grid was taken in Y-direction. On the other hand non-uniform grids were taken in the X-direction. The discretization equations were solved by the Gauss-Seidel method. The iteration method used in this program is a line-by-line procedure, which is a combination of the direct method and the resulting Tri Diagonal Matrix Algorithm (TDMA). The accuracy was defined by the change in the average Nusselt number through one hundred iterations to be less than 0.01 % from its value. The check showed that 3500 iterations were enough for all of the investigated values.

4. Program validation and comparison with previous research

In order to check on the accuracy of the numerical technique employed for the solution of the problem considered in the present study, it was validated by performing simulation for double-diffusive convection flow in a vertical rectangular enclosure with combined horizontal temperature and concentration gradients and in the presence of magnetic field and heat generation effects which were reported by Chamkha and Al-Naser [23]. Fig. 2 plots the predicted values for average Nusselt numbers over a range for Hartmann from 0 to 50 for the present solution and the results published by Chamkha and Al-Naser [23]. In the figure, the heat generation coefficient equals to zero and one. The following parameters were kept constant N=–0.8, Gr_T =10^5, Pr=1, Le=2 and A=2. In addition, fig. 3 plots the values of the average Sherwood number for the same previous conditions. The maximum deviation between the results through this range was within two percent. Some of this deviation may be from the accuracy in the measuring from the graphs or from the solution techniques. Also, fig. 4-a and b present comparisons for the isotherms, concentration contours, density and streamlines contours of the present work at N =- 0:8, Ra_T=10^5, Ha=25, Pr=1, Le=2 and φ=0 and Chamkha and Al-Naser [23]. The figure shows good agreement.

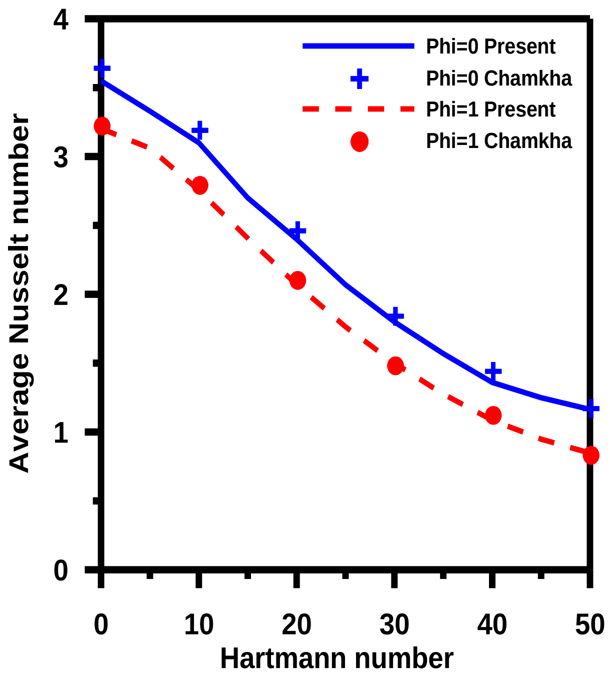

Fig. 2. Comparison for average Nusselt number with Chamkha and Al-Naser [23] results, N=–0.8, Gr_T =10^5, Pr=1, Le=2 and A=2.

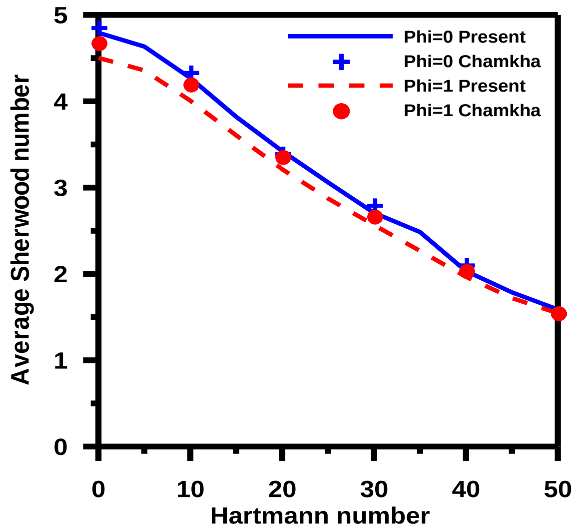

Fig. 3. Comparison for average Sherwood number with Chamkha and Al-Naser [23] results, N=–0.8, Gr_T =10^5, Pr=1, Le=2 and A=2.

5. Results and discussion

In this study, the Prandtl number, Pr is kept constant at Pr = 0.7, aspect ratio, A=2 and Le=1. The base case in this study is made with thermal Rayleigh number Ra_T=10^6, Hartmann number Ha=50 buoyancy ratio N=1 and dimensionless heat generation φ=1. The numerical results for the streamline, density, isothermals and isoconcentration contours for various values of thermal Rayleigh number Ra_T, Hartmann number Ha, Buoyancy ratio N, and the heat generation or absorption coefficient φ, will be presented and discussed. In addition, the results for both average Nusselt, and average Sherwood numbers, at various conditions will be presented and discussed.

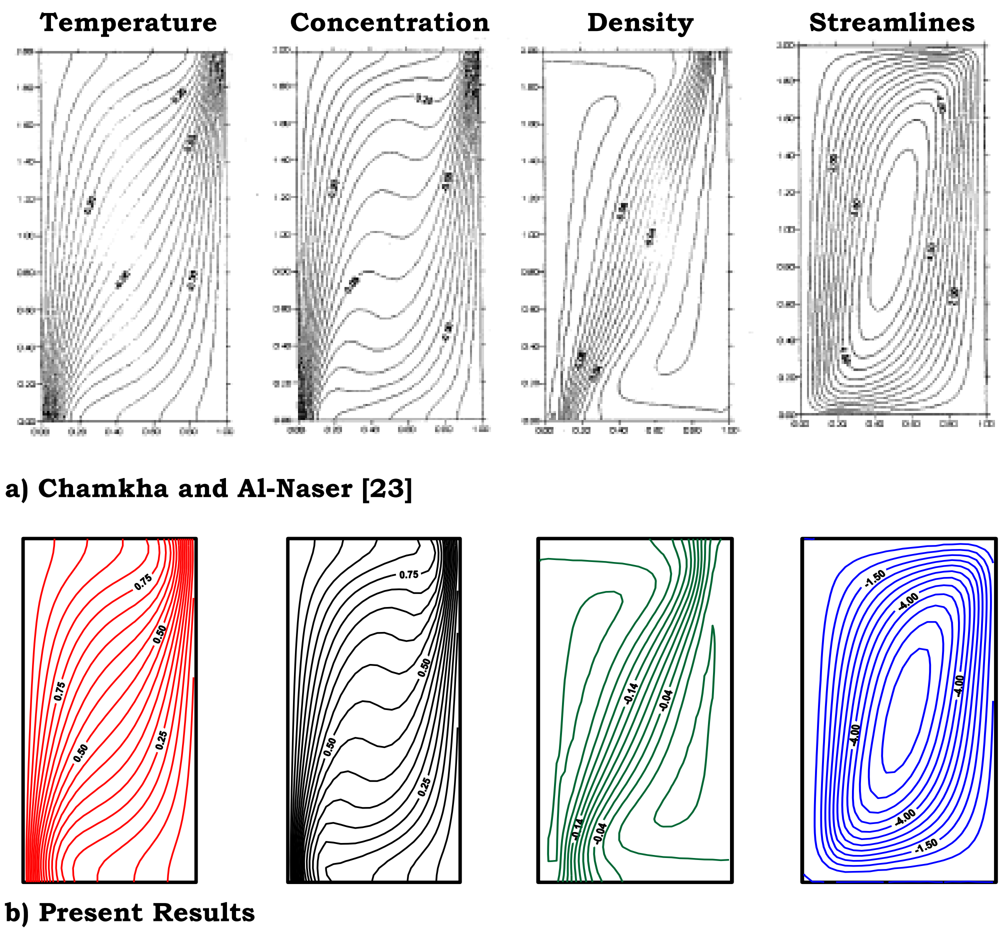

Fig. 4. Comparison with Chamkha and Al-Naser [23], Ra_T=10^5, Ha=25, Pr=1, Le=2 and φ=0.

Fig. 5 presents the effect of thermal Rayleigh number on the streamline, density, isothermals and isoconcentration contours for Hartmann number Ha=50, Le=1, Pr=0.7, N=1 and φ=1. In this figure the effect of both thermal buoyancy force and solutal buoyancy force are equal. Therefore, the double diffusive flow is applicable. In addition φ=1, a heat generation is also considered. For low thermal Rayleigh number Ra_T=10^3, the conduction regime is dominant. The isotherms and isoconcentration are parallel lines. These lines are parallel to the vertical cavity walls. Also, the dimensionless density lines are parallel. The flow consists of a very weak clockwise cell with maximum strength ψ_{max}= 0.1. Also, it can be seen from the figure an equal spacing separates the isoconcentration lines. On the other hand a non-equal spacing separates the isothermal lines, a wider gab is observed near the hot wall. In ordinary double diffusive flow with out magnetic field nor heat generation nor absorption, the isothermals and isoconcentrations must be similar for Le=1. But in our condition, if a heat source is imposed, it is opposing the heat flow from hot wall. Moreover, the cold wall receives much heat than that input by the hot one. Therefore, near the hot wall, the value of temperature gradient is less than that near the cold wall. As the thermal Rayleigh number is increased Ra_T=10^4, the convection mode is pronounced, the flow cell becomes stronger with maximum strength Ψ_{max}=1. Since, the cell is coming to the hot wall from the cavity bottom and depart from it at the cavity top, both heat and mass transfer at the cavity bottom is higher than at the top. The figure shows, the isothermals and concentrations are closer to the hot wall in the lower region. Furthermore, the effect of heat generation already exists, as mentioned above; the temperature gradient is smaller than the concentration gradient. At thermal Rayleigh number 10^6, the convection is dominant, the circulating cell is very strong with maximum strength Ψ_{max}=24. The streamlines are crowded near the cavity wall and the cavity core is empty. As well as both isothermals and isoconcentrations are stratified in vertical direction except near the insulated surfaces of the enclosure and appear as horizontal lines in the cavity core. In addition, the heat generation hasn't any significant effect.

Fig. 6 illustrates the effect of Hartmann number Ha, on the streamlines, density, isothermals and isoconcentrations contours. To highlight on the effect of Ha, the thermal Rayleigh number is kept constant Ra_T=10^6, Pr=0.7, Le=1, N=1 and φ=1. Without magnetic field Ha=0, a very strong clockwise cell is observed as well as the streamlines are very crowded near the vertical walls. Also it is seen horizontal distributions for density, isothermal and concentrations in the cavity core. As the magnetic field is imposed Ha=20, the flow strength slightly reduces and the streamlines penetrates slightly to the cavity core. In addition two small cells appear at the middle cavity height, one in each side. As the Hartmann number increases, the flow strength is damped more, the small cells disappeared, and the streamlines penetrate more towards the cavity center. Consequently, a reduction on the temperature and concentration gradients near the cavity wall and they are tilted upward in the cavity core

The effect of heat generation or absorption coefficient inside the cavity φ, on the different contours is shown in fig. 7 for Ra_T=10^6, Pr=0.7, Le=1, N=1 and Ha=50. Without heat source or sink φ=0, the flow is one big central clockwise cell, the flow moves upwards near the hot wall and downwards near the cold one. In addition, the density, isothermals and isoconcentrations are horizontal lines in the cavity core. As heat absorbed is applied φ<0, according to the conservation of energy law; the rate of heat transfer from the hot wall is higher than the rate of heat received by the cold one. so the fluid velocity near hot wall is higher than that near the cold one. Consequently, the hot wall attracts the cell in the left direction. Furthermore, the temperature gradient increases near the hot wall and the isothermal shifted upwards. As the heat absorption coefficient increases, the cell shifts slightly upwards and more towards to hot wall as well as the isothermals moves upwards. On the other hand, the density contour doesn't change. The heat absorption has a minor effect on the isoconcentrations especially at the upper portion of the cavity,

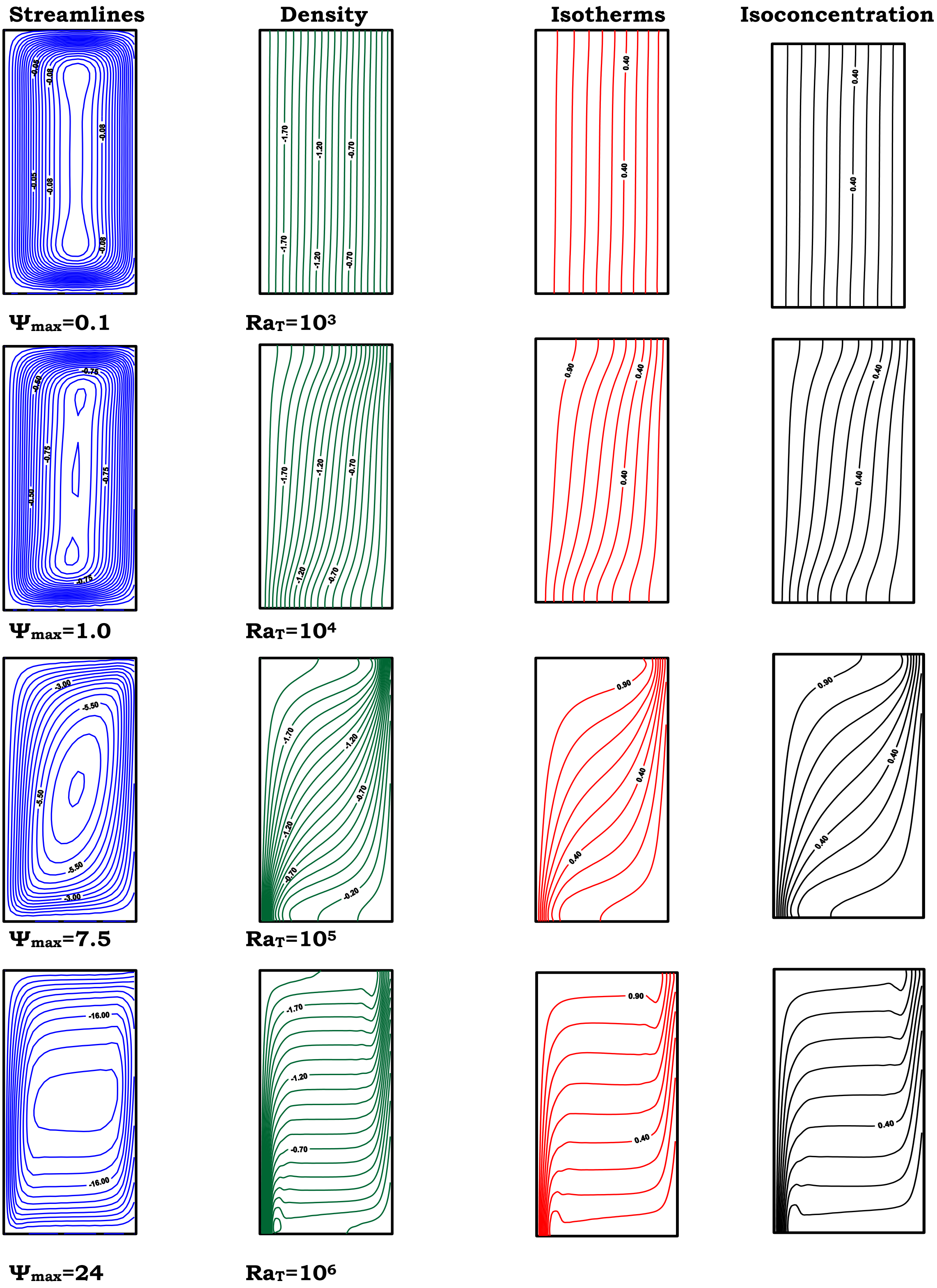

Fig. 5. Effect of Thermal Rayleigh number on Streamlines, Density, Isotherms and Isoconcentration. Ha=50, Le=1, N=1 and φ=1.

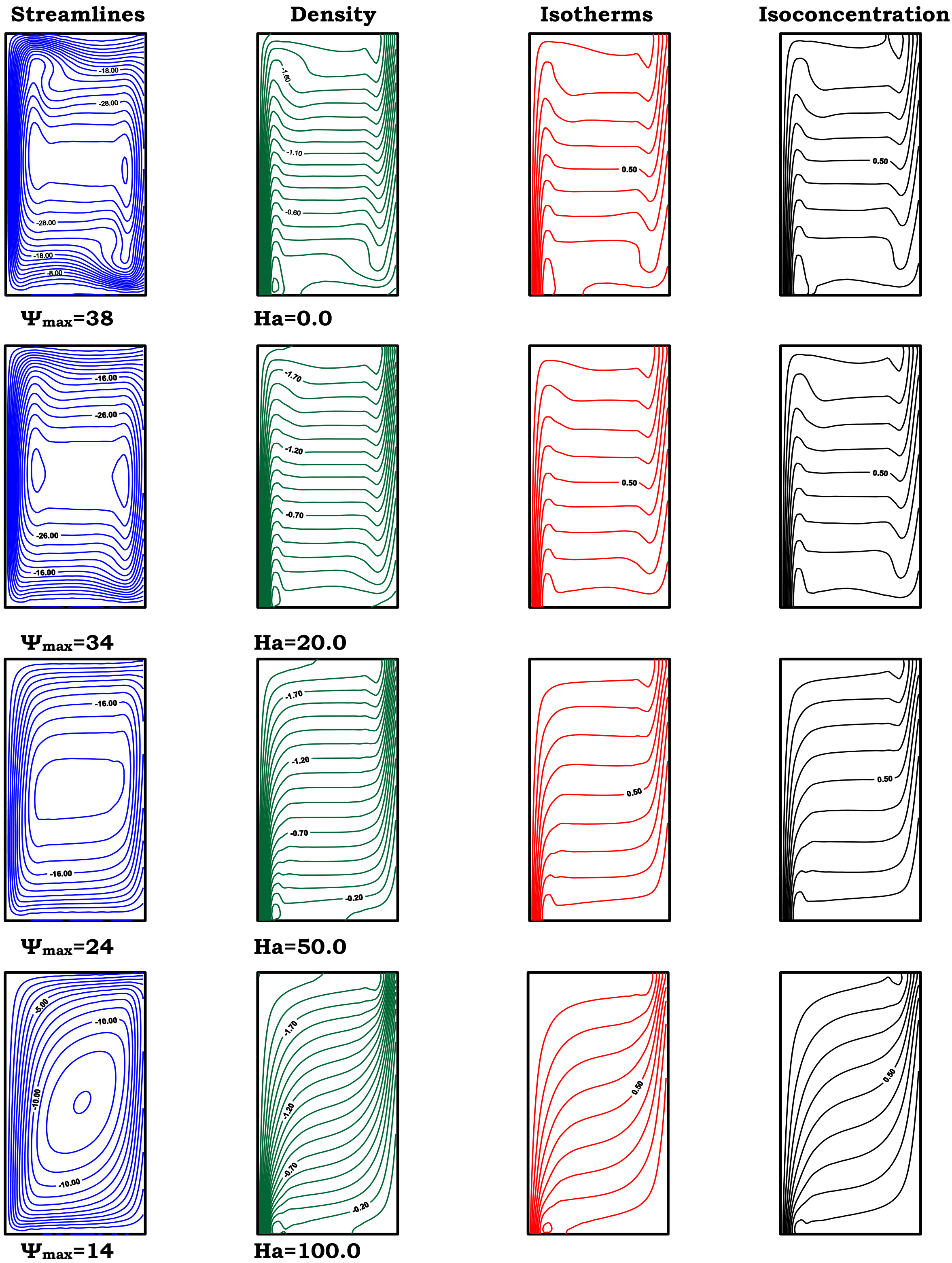

Fig. 6. Effect of Hartmann number on Streamlines, Density, Isotherms and Isoconcentration. $Ra_T=10^6$, Le=1, N=1 and φ=1.

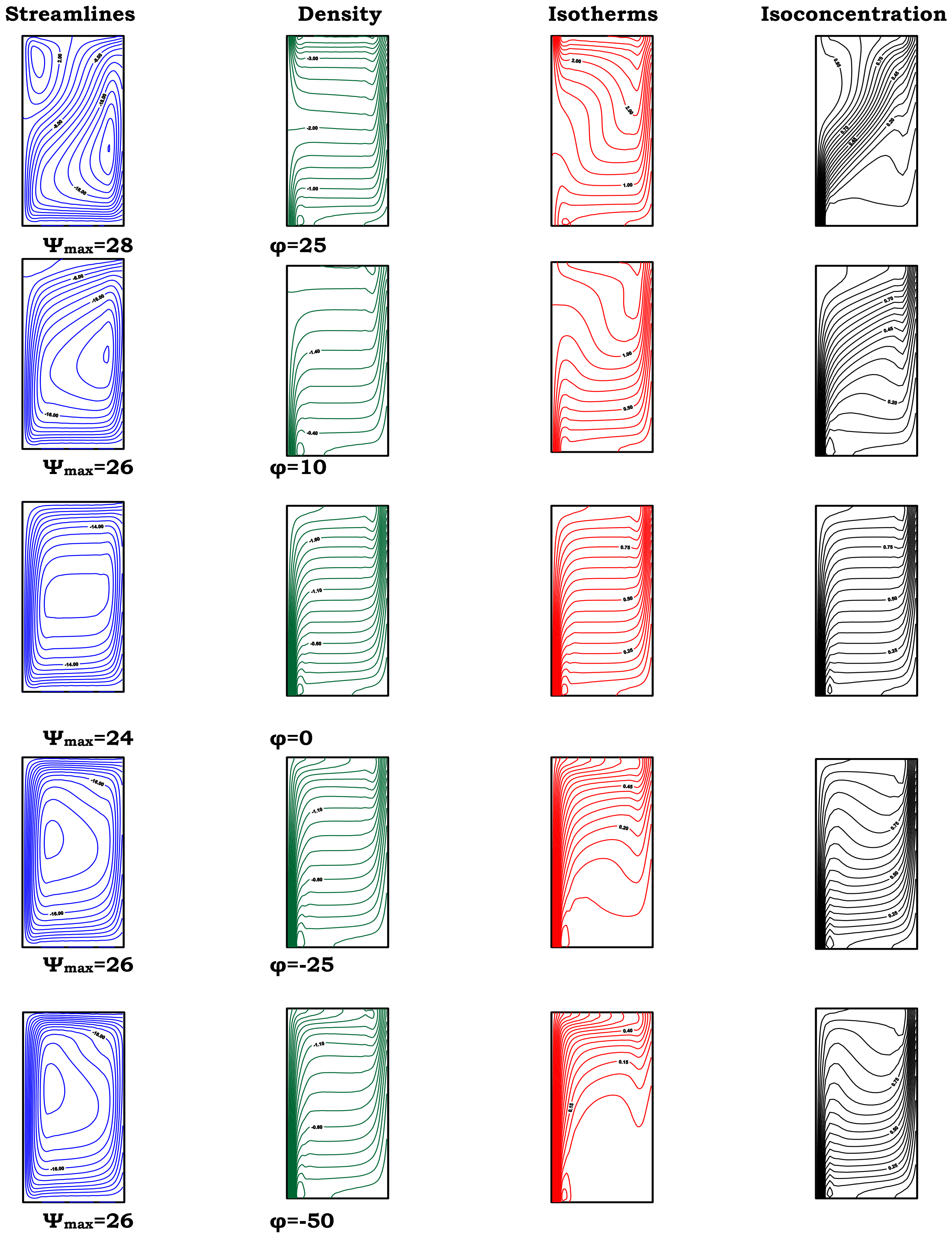

Fig. 7. Effect of Heat generation or absorption on Streamlines, Density, Isotherms and Isoconcentration. $Ra_T=10^6$, Le=1, N=1 and Ha=50.

which has a strong flow, the straight lines is destroyed. The presence of heat source within the enclosure $\varphi>0$, causes an increase in the fluid temperature. So the heat transfer from the hot wall is reduced and the heat transfer to the cold is increased. So the cell is shifted right. As the heat generation increases, the fluid temperature increases and reaches more than the hot wall temperature in the upper portion of the cavity. Therefore, the direction of heat transfer reverses and become from the fluid to the hot wall. Consequently, a counterclockwise small cell appeared at the upper left corner. In addition a concentration plume from left lower part is noticed. It is interesting to explore the effect of these phenomena on the distribution for both local Nusselt and Sherwood numbers over the hot wall. Figs. 8 and 9 represent these distributions. In general, the local Nusselt number has maximum values at the cavity bottom and it's value decreases as we move upwards. The local Nusselt number decreases as φ increases. For strong heat source φ=25, the local Nusselt has a negative value at the upper section of the cavity. This means that, the heat is transferred from the fluid to the hot wall. The sign of the local Nusselt changes when the small counterclockwise cell appears. If we return to fig. 7 it is noticeable that the absolute value for the temperature gradient has a maximum value at this position, since this cell is coming to the hot wall at the upper corner. Consequently, the absolute value for local Nusselt has maximum value. This also can be observed from the high density of the isothermal contours at this section. On the other hand, the heat source or sink have no significant effect on the local Sherwood number.

The combined effect of thermal Rayleigh number and Hartmann number on the average Nusselt and Sherwood numbers is presented in figs. 10 and 11 for Le=1, Pr=0.7, φ=1 and N=1. Without imposing the magnetic flux Ha=0, both average Nusselt and Sherwood numbers increases with the thermal Rayleigh number. In addition, for the same value of thermal Rayleigh number, as the magnetic field is increased both average Nusselt and Sherwood numbers decreases. Furthermore, at Hartmann number Ha>20, both the average Nusselt and Sherwood numbers have constant values over a range of thermal Rayleigh number. This range increases with increasing Hartmann number. It is interesting to note that this phenomenon was detected experimentally by Ujihara et al. [1].

The combined effect for the magnetic field and heat source or sink on both average Nusselt and Sherwood numbers is illustrated in figs. 12 and 13. For constant $Ra_T=10^6$, Le=1, Pr=0.7 and N=1. It is observed that both Nu and Sh have a decreasing trend with increases in Hartmann number. In addition, it is observed that heat generation ($\varphi>0$) decreases the average Nusselt number while heat absorption ($\varphi<0$) increases it. However, both heat generation ($\varphi>0$) and heat absorption ($\varphi<0$), slightly decrease the average Sherwood number. As expected, the effect of the heat generation or absorption coefficient φ is more pronounced on the values of Nusselt than on Sherwood. Moreover, for heat source with high coefficient, the sign of the average Nusselt number is changed from positive to negative.

The influence of the buoyancy ratio N on the average Nusselt and Sherwood numbers for different Hartmann number is shown in figs. 14 and 15 respectively, for $Ra_T=10^6$, Le=1 and φ=1. It is interesting to observe from these figures the existence of minimum values in both average Nusselt and Sherwood numbers for a buoyancy ratio of about -1. The values of Nu and Sh tend to increase with increasing the absolute values of Buoyancy ratio. The existence of such minimum values in Nusselt and Sherwood has been reported in the literature.

6. Conclusions

Steady heat and mass transfer by natural convection flow of a heat generating fluid inside a rectangular enclosure in the presence of a transverse magnetic field was studied numerically. The finite-difference method was employed for the solution of the present problem. Comparisons with previously published work on special cases of the problem were performed and found to be in good agreement. Graphical results for various

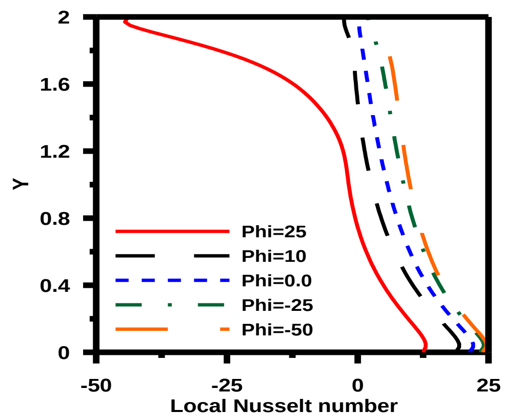

Fig. 8. Effect of heat generation or absorption coefficient φ, on local Nusselt number, Ra_T=10^6, Le=1, N=1 and Ha=50.

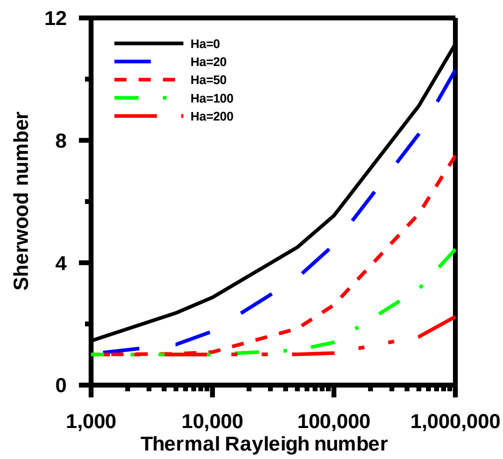

Fig. 11. Sherwood number vs. Ra_T for different Ha, Le=1, φ=1 and N=1.

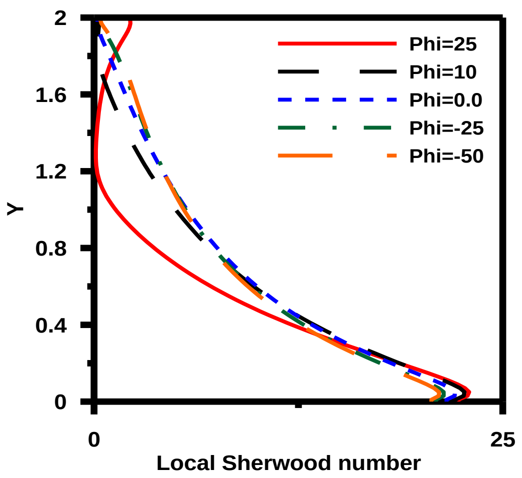

Fig. 9. Effect of heat generation or absorption coefficient φ, on local Sherwood number, Ra_T=10^6, Le=1, N=1 and Ha=50.

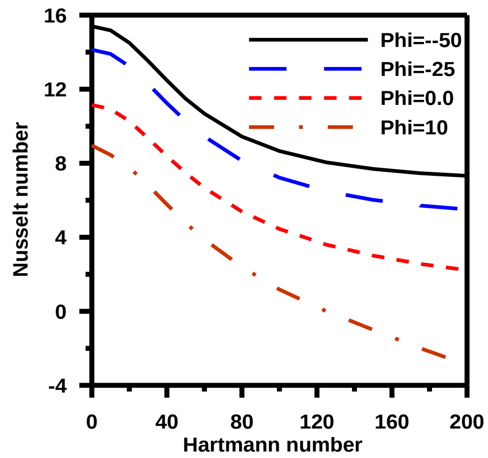

Fig. 12. Nusselt number vs. Hartmann number for different φ, Ra_T=10^6, Le=1 and N=1.

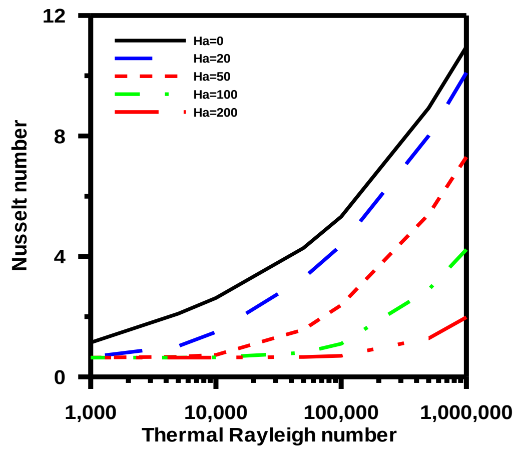

Fig. 10. Nusselt number vs. Ra_T for different Ha, Le=1, φ=1 and N=1.

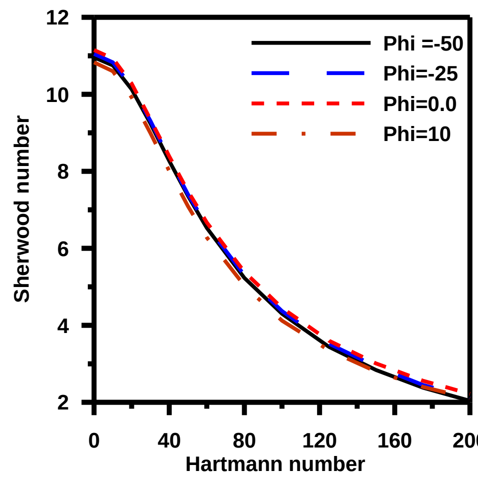

Fig. 13. Sherwood number vs. Hartmann number for different φ, Ra_T=10^6, Le=1 and N=1.

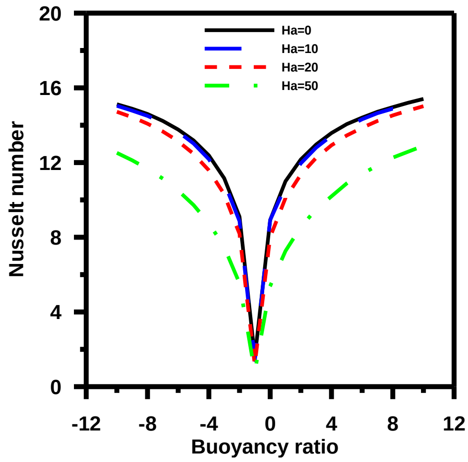

Fig. 14. Average Nusselt number vs. buoyancy ratio for different Hartmann numbers, Ra_T=10^6, Le=1 and φ=1.

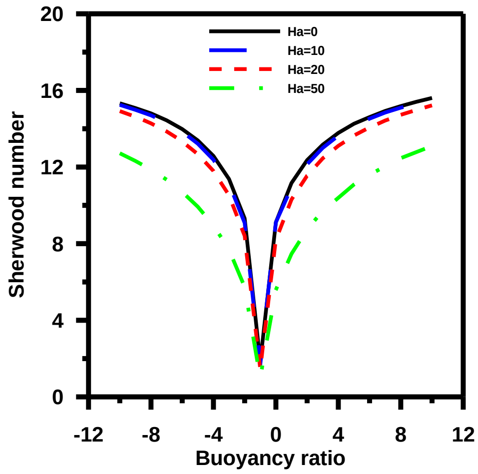

Fig. 15. Average Sherwood number vs. buoyancy ratio for different Hartmann numbers, Ra_T=10^6, Le=1 and φ=1.

parametric conditions were presented and discussed. The study revealed the following;

1. The heat and mass transfer mechanisms and the flow characteristics inside the enclosure depended strongly on the strength of the magnetic field and heat generation or absorption effects.
2. The magnetic field was found to reduce the heat transfer and fluid circulation within the enclosure.
3. The average Nusselt number was increased in the presence of a heat sink while it was decreased when a heat source was present.
4. The sign of the average Nusselt number was changed from positive to negative in the case of high heat generation.
5. The presence of heat source or heat sink slightly reduces the average Sherwood number.
6. For Hartmann number Ha>20, both the average Nusselt and Sherwood numbers have constant values over a range of thermal Rayleigh number, this range increases with increasing Hartmann number.
7. The average Nusselt and Sherwood numbers have minimum values at buoyancy ratio N=1.
8. Over the investigated range for this study, the periodic oscillatory behavior in the stream function wasn't observed. The effect of both Prandtl and Lewis are very important in this subject. So, in the future, we should explore the effect of Pr and Le.

Nomenclature

A	is the aspect ratio, H/L,
B_o	is the magnetic induction, Tesla = N/Amp.m^2,
c	is the vapour concentration,
c_h, c_l	is the concentrations at the left, and the right walls of the cavity, respectively,
C	is the dimensionless vapour concentration, $C=(c-c_l)/(c_h-c_l)$,
D	is the mass diffusivity, m^2/s,
g	is the acceleration of gravity, m/s^2,
Gr_S	is the solutal Grashof number based on the half width of the cavity, $Gr_S = g\beta(c_h-c_l)L^3/\nu^2$,
Gr_T	is the thermal Grashof number based on the half width of the cavity, $Gr_T = g\beta(T_h-T_c)L^3/\nu^2$,
h	is the heat transfer coefficient , W/m^{2}K,
h_s	is the solutal transfer coefficient, m/s,
H	is the cavity height, m,
Ha	is the Hartmann number, $B_o L\sqrt{\sigma/\mu}$,
k	is the fluid thermal conductivity, W/m K,
L	is the cavity width, m,
Le	is the Lewis number, Le= $a/D=Sc/Pr$,
N	is the Buoyancy ratio, $N = \beta_S \Delta C / \beta\Delta T$, or $N=Ra_S/Ra_T$,
Nu	is the average Nusselt number, $Nu = hL/k$,

Nu_i is the local Nusselt number, $Nu_i = -(\partial\theta / \partial X)_{X=0}$,
p is the pressure, N / m^2,
P is the dimensionless pressure, $P = pH_o^2/\rho_o \alpha^2$,
Pr is the Prandtl number, $Pr = \nu / \alpha$,
Q_o is the heat generation or absorption coefficient, Watt/m^3.^{o}C,
Ra_S is the solutal Rayleigh number, $Ra_S = Gr_S * Pr$,
Ra_T is the thermal Rayleigh number, $Ra_T = Gr_T * Pr$,
Sc is the Schmidt number, Sc= ν/D,
Sh is the Average Sherwood number, $Sh = h_s L / D$,
Sh_i is the local Sherwood number, $Sh_i = -(\partial C / \partial X)_{Y=0}$,
T is the local temperature, K,
T_h , T_c is the hot and cold wall temperatures respectively, K,
ΔT is the temperature difference, ($T_h - T_c$), K,
u , v is the velocity components in the x and y directions respectively, m/s,
U , V is the dimensionless velocity components in the X and Y directions respectively, ($U = uL/\alpha$ and $V = vL/\alpha$),
x, y is the dimensional coordinates, m, and
X,Y is the dimensionless coordinates, $X=x/L$ and $Y=y/L$.

Greek symbols

α is the thermal diffusivity, m^2/s,
β_T is the coefficient of thermal expansion, K^{-1},
β_S is the coefficient of solutal expansion, Kg^{-1},
Φ is the dimensionless heat generation or absorption, $Q_o L^2 / \rho c_p \alpha$,
θ is the dimensionless temperature, ($T - T_c$) / ($T_h - T_c$),
μ is the dynamic viscosity, kg/m.s,
ν is the Kinematics viscosity, m^2/s,
ρ is the local fluid density, Kg/m^3,
ρ_o is the fluid density at the bottom surfaces, Kg/m^3,
ρ^* is the Dimensionless density= NC-θ,
σ is the electrical conductivity, Amp.m/Volt,
Ψ is the dimensionless stream function, and
Ψ_{max} is the maximum dimensionless stream function.

References

[1] A. Ujihara, T. Tagawa and H. Ozoe, "Average Heat Transfer Rates Measured in two Different Temperature Ranges for Magnetic Convection of Horizontal Water Layer Heated from Below", International Journal of Heat and Mass Transfer, Vol. 49, Article in Press (2006).

[2] S. Ostrach, "Natural Convection with Combined Driving Forces", Physico Chem. Hydrodyn, Vol. 1, pp. 233–247 (1980).

[3] S. Acharya and R.J. Goldstein, "Natural Convection in an Externally Heated Square Box Containing Internal Energy Sources", J. Heat Transfer, Vol. 107, pp. 855–866 (1985).

[4] M. Rahman and M.A.R Sharif. "Numerical Study of Laminar Natural Convection in Inclined Rectangular Enclosures of Various Aspect Ratios", Numer. Heat Transfer A, Vol. 44, pp. 355–373 (2003).

[5] H. Oztop and E. Bilgen, "Natural Convection in Differentially Heated and Partially Divided Square Cavities with Internal Heat Generation", International Journal of Heat and Fluid Flow, Vol. 27, pp. 466–475 (2006).

[6] S.V. Patankar, Numerical Heat Transfer and Fluid Flow, McGraw-Hill, New York (1980).

[7] Y. Shu, B.Q. Li and H.C. de Groh, "Magnetic Damping of G-Jitter Induced Double-Diffusion Convection", Num. Heat Transfer, Part A, Vol. 42, pp. 345–364 (2002).

[8] H. Ozoe and K. Okada, "The Effect of the Direction of the External Magnetic Field on the Three-Dimensional Natural Convection in A Cubic Enclosure", Int. J. Heat Mass Transfer, Vol. 32, pp. 1939–1953 (1989).

[9] T. Alboussie`re, J.P. Garandet and R. Moreau, "Asymptotic Analysis and Symmetry in MHD Convection", Phys., Fluids, Vol. 8, pp. 2215–2226 (1996).

[10] N.I. Wakayama, "Behavior of Flow under Gradient Magnetic Field", J. Appl. Phys., Vol. 69 (4), pp. 2734–2736 (1991).

[11] B. Bai, A. Yabe, J. Qi and N.I. Wakayama, "Quantitative Analysis of Air Convection Caused By Magnetic–Fluid Coupling", AIAA J., Vol. 37 (12), pp. 1538–1543 (1999).

[12] T. Tagawa, R. Shigemitsu and H. Ozoe, "Magnetizing Force Modeled and Numerically Solved for Natural Convection of Air in a Cubic Enclosure: Effect of the Direction of the Magnetic Field", Int. J. Heat Mass Transfer, Vol. 45, pp. 267–277 (2002).

[13] M. Kaneda, T. Tagawa and H. Ozoe, "Convection Induced By a Cuspshaped Magnetic Field for Air in a Cube Heated from Above and Cooled from Below", J. Heat Transfer, Vol. 124, pp. 17–25 (2002).

[14] B. Xu, B.Q. Li and D.E. Stock, "An Experimental Study of Thermally Induced Convection of Molten Gallium in Magnetic Fields", International Journal of Heat and Mass Transfer, Vol. 49, pp. 2009–2019 (2006).

[15] J. I. Morton, N. Ma, D.F. Bliss and G.G. Bryant, "Dopant Segregation during Liquid-Encapsulated Czochralski Crystal Growth in A Steady Axial Magnetic Field", Journal of Crystal Growth, Vol. 242, pp. 471–485 (2002).

[16] J.F. Kuniholm and N. Ma, "Natural Convection in a Liquid Encapsulated Molten Semiconductor with a Steady Magnetic Field", International Journal of Heat and Fluid Flow, Vol. 24, pp. 130–136 (2003).

[17] M. Yang and N. Ma, "A Computational Study of Natural Convection in A Liquid-Encapsulated Molten Semiconductor with A Horizontal Magnetic Field", International Journal of Heat and Fluid Flow, Vol. 26, pp. 810–816 (2005).

[18] X. Wang, N. Ma, D.F. Bliss, G.W. Iseler and P. Becla, "Comparing Modified Vertical Gradient Freezing with Rotating Magnetic Fields or with Steady Magnetic and Electric Fields", J. Cryst. Growth, Vol. 287, pp. 270–274 (2006).

[19] X. Wang, N. Ma, D.F. Bliss and G.W. Iseler, "Semiconductor Crystal Growth by Modified Vertical Gradient Freezing With Electromagnetic Stirring", J. Thermophys. Heat Transfer, Vol. 19, pp. 95–100 (2005).

[20] A.M. Holmes, X. Wang, N. Ma, D.F. Bliss and G.W. Iseler, "Vertical Gradient Freezing Using Submerged Heater Growth with Rotation and with Weak Magnetic and Electric Fields", Int. J. Heat Fluid Flow, Vol. 26, pp. 792–800 (2005).

[21] X. Wang, N. Ma, D.F. Bliss and G.W. Iseler, "A Numerical Investigation of Dopant Segregation by Modified Vertical Gradient Freezing with Moderate Magnetic and Weak Electric Fields", Int. J. Eng. Sci, Vol. 43, pp. 908–924 (2005).

[22] T. Nishimura, M. Wakamatsu and A. M. Morega, "Oscillatory Double-Diffusive Convection in a Rectangular Enclosure with Combined Horizontal Temperature and Concentration Gradients", International Journal of Heat and Mass Transfer, Vol. 41, pp. 1601–1611 (1998).

[23] A.J. Chamkha and H. Al-Naser, "Hydromagnetic Double-Diffusive Convection in A Rectangular Enclosure with Opposing Temperature and Concentration Gradients", International Journal of Heat and Mass Transfer, Vol. 45, pp. 2465–2483 (2002).

[24] A.J. Chamkha and H. Al-Naser, "Hydromagnetic Double-Diffusive Convection in A Rectangular Enclosure with Uniform Side Heat and Mass Fluxes and Opposing Temperature and Concentration Gradients", International Journal of Thermal Sciences, Vol. 41, pp. 936–948 (2002).

Received June 24, 2006
Accepted July 29, 2006